Video Article

Au-Interaction of Slp1 Polymers and Monolayer from *Lysinibacillus sphaericus* JG-B53 - QCM-D, ICP-MS and AFM as Tools for Biomolecule-metal Studies

Matthias Suhr[1], Johannes Raff[1,2], Katrin Pollmann[1]

[1]Helmholtz Institute Freiberg for Resource Technology, Helmholtz-Zentrum Dresden-Rossendorf

[2]Institute for Resource Ecology, Helmholtz-Zentrum Dresden-Rossendorf

Correspondence to: Matthias Suhr at m.suhr@hzdr.de

URL: https://www.jove.com/video/53572
DOI: doi:10.3791/53572

Keywords: Chemistry, Issue 107, Biosorption, metals, S-layer, bacteria, nanoparticles, QCM-D, AFM, ICP-MS, gold

Date Published: 1/19/2016

Citation: Suhr, M., Raff, J., Pollmann, K. Au-Interaction of Slp1 Polymers and Monolayer from *Lysinibacillus sphaericus* JG-B53 - QCM-D, ICP-MS and AFM as Tools for Biomolecule-metal Studies. *J. Vis. Exp.* (107), e53572, doi:10.3791/53572 (2016).

Abstract

In this publication the gold sorption behavior of surface layer (S-layer) proteins (Slp1) of *Lysinibacillus sphaericus* JG-B53 is described. These biomolecules arrange in paracrystalline two-dimensional arrays on surfaces, bind metals, and are thus interesting for several biotechnical applications, such as biosorptive materials for the removal or recovery of different elements from the environment and industrial processes. The deposition of Au(0) nanoparticles on S-layers, either by S-layer directed synthesis [1] or adsorption of nanoparticles, opens new possibilities for diverse sensory applications. Although numerous studies have described the biosorptive properties of S-layers [2-5], a deeper understanding of protein-protein and protein-metal interaction still remains challenging. In the following study, inductively coupled mass spectrometry (ICP-MS) was used for the detection of metal sorption by suspended S-layers. This was correlated to measurements of quartz crystal microbalance with dissipation monitoring (QCM-D), which allows the *online* detection of proteinaceous monolayer formation and metal deposition, and thus, a more detailed understanding on metal binding.

The ICP-MS results indicated that the binding of Au(III) to the suspended S-layer polymers is pH dependent. The maximum binding of Au(III) was obtained at pH 4.0. The QCM-D investigations enabled the detection of Au(III) sorption as well as the deposition of Au(0)-NPs in real-time during the *in situ* experiments. Further, this method allowed studying the influence of metal binding on the protein lattice stability of Slp1. Structural properties and protein layer stability could be visualized directly after QCM-D experiment using atomic force microscopy (AFM). In conclusion, the combination of these different methods provides a deeper understanding of metal binding by bacterial S-layer proteins in suspension or as monolayers on either bacterial cells or recrystallized surfaces.

Video Link

The video component of this article can be found at https://www.jove.com/video/53572/

Introduction

Due to the increasing use of gold for several applications like electronics, catalysts, biosensors, or medical instruments, the demand of this precious metal has grown over the last few years' time [6-9]. Gold as well as many other precious and heavy metals are released into the environment via industrial effluents in dilute concentrations, through mining activities, and waste disposal [7,8,10],although most environmental contamination by heavy or precious metals is an on-going process mainly caused by technological activities. This leads to a significant interference of natural ecosystems and could potentially threaten human health [9]. Knowing these negative outcomes promotes the search for new techniques to remove metals from contaminated ecosystems and improvements in recycling metals from industrial wastewater. Well-established physico-chemical methods like precipitation or ion exchange are not so effective, especially in highly diluted solutions [7,8,11]. Biosorption, either with living or dead biomass, is an attractive alternative for wastewater treatment [10,12]. The use of such biological materials can reduce the consumption of toxic chemicals. Many microorganisms have been described to accumulate or immobilize metals. For instance, cells of *Lysinibacillus sphaericus* (*L. sphaericus*) JG-A12 have shown high binding capacities for precious metals, *e.g.,* Pd(II), Pt(II), Au (III), and other toxic metals like Pb(II) or U(VI) [4,13], cells of *Bacillus megaterium* for Cr(VI) [14], cells of *Saccharomyces cerevisiae* for Pt(II) and Pd(II) [15], and *Chlorella vulgar for* Au(III) and U(VI) [16,17]. The binding of previous metals like Au(III), Pd(II), and Pt(II) has also been reported for *Desulfovibrio desulfuricans*[18] and for *L. sphaericus* JG-B53 [19,20]. Nevertheless, not all microbes bind high amounts of metals and their application as sorptive material is limited [12,21]. Furthermore, metal binding capacity depends on different parameters, *e.g.,* cell composition, the used bio-component, or environmental and experimental conditions (pH, ionic strength, temperature etc.). The study of isolated cell wall fragments [22,23], like membrane lipids, peptidoglycan, proteins, or other components, helps to understand the metal binding processes of complex constructed whole cells [8,21].

The cell components focused on in this study are S-layer proteins. S-layer proteins are parts of the outer cell envelope of many bacteria and archaea, and they constitute about 15 - 20% of the total protein mass of these organisms. As the first interface to the environment, these cell compounds strongly influence the bacterial sorption properties [3]. S-layer proteins with molecular weights ranging from forty to hundreds of

kDa are produced within the cell, but are assembled outside where they are able to form layers on the lipid membranes or polymeric cell wall components. Once isolated, nearly all S-layer proteins have the intrinsic property to spontaneously self-assemble in suspension, at interfaces, or on surfaces forming planar or tube-like structures [3]. The thickness of the protein monolayer depends on the bacteria and is within a range of 5 - 25 nm [24]. In general, the formed S-layer protein structures can have an oblique (*p1* or *p2*), square (*p4*), or hexagonal (*p3* or *p6)* symmetry with lattice constants of 2.5 to 35 nm [3,24]. The lattice formation seems to be in many cases dependent on divalent cations and mainly on Ca^{2+} [25,26, Raff, J. et al. S-layer based nanocomposites for industrial applications in Protein-based Engineered Nanostructures. (eds Tijana Z. Grove & Aitziber L. Cortajarena) (Springer, 2016 (submitted))].

Nevertheless, the full reaction cascade of monomer folding, monomer-monomer interaction, the formation of a lattice, and the role of different metals, especially of divalent cations such as Ca^{2+} and Mg^{2+}, are still not fully understood.

The gram-positive strain *L. sphaericus* JG-B53 (renamed from *Bacillus sphaericus* after new phylogenetic classification) [27] was isolated from the uranium mining waste pile "Haberland" (Johanngeorgenstadt, Saxony, Germany) [4,28,29]. Its functional S-layer protein (Slp1) possesses a square lattice, a molecular weight of 116 kDa [30], and a thickness of ≈ 10 nm on living bacteria cells [31]. In previous studies, the *in vitro* formation of a closed and stable protein layer with a thickness of approximately 10 nm was achieved in less than 10 min [19]. The related strain *L. sphaericus* JG-A12, also an isolate from the "Haberland" pile, possesses high metal binding capacities and its isolated S-layer protein has shown a high chemical and mechanical stability and good sorption rates for precious metals like Au(III), Pt(II), and Pd(II) [4,32,33]. This binding of precious metals is more or less specific for some metals and depends on the availability of functional groups on the outer and inner protein surface of the polymer and in its pores, ionic strength, and the pH value. Relevant functional groups for metal interaction by the proteins are COOH-, NH_2-, OH-, PO_4-, SO_4-, and SO-. In principle, metal binding capacities open a wide spectrum of applications, [Raff, J. et al. S-layer based nanocomposites for industrial applications in Protein-based Engineered Nanostructures. (eds Tijana Z. Grove & Aitziber L. Cortajarena) (Springer, 2016 (submitted))] *e.g.,* as biosorptive components for removal or recovery of dissolved toxic or valuable metals, templates for synthesis or defined deposition of regularly structured metallic nanoparticles (NPs) for catalysis, and other bio-engineered materials like bio-sensory layers [3,5,18,33]. Regularly arranged NP arrays like Au(0)-NPs could be used for major applications ranging from molecular electronics and biosensors, ultrahigh density storage devices, and catalysts for CO-oxidation [34-37]. The development of such applications and smart design of these materials necessitates a deeper understanding of the underlying metal binding mechanisms.

A prerequisite for the development of such bio-based materials is the reliable implementation of an interface layer between the biomolecule and the technical surface [38,39]. For example, polyelectrolytes assembled with the layer-by-layer (LbL) technique [40,41] have been used as an interface layer for recrystallization of S-layer proteins [39]. Such an interface offers a relatively easy way to perform the protein coating in a reproducible and quantitative way. By performing different experiments with and without modification with adhesive promoters, it is possible to make statements regarding coating kinetics, layer stability, and interaction of metals with biomolecules [19,42,Raff, J. et al. S-layer based nanocomposites for industrial applications in Protein-based Engineered Nanostructures. (eds Tijana Z. Grove & Aitziber L. Cortajarena) (Springer, 2016 (submitted))]. However, the complex mechanism of the protein adsorption and protein-surface interaction is not completely understood. Especially information on conformation, pattern orientation, and coating densities is still missing.

Quartz crystal microbalance with dissipation monitoring (QCM-D) technique has attracted attention in the recent years as a tool for studying protein adsorption, coating kinetics, and interaction processes on the nanometer scale [19,43-45]. This technique allows for the detailed detection of mass adsorption in real-time, and can be used as an indicator for the protein self-assembling process and coupling of functional molecules on protein lattices [19,20,42,46-48]. In addition, QCM-D measurements open the possibility to study metal interaction processes with the proteinaceous layer under natural biological conditions. In a recent study, the interaction of the S-layer protein with selected metals like Eu(III), Au(III), Pd(II),and Pt(II) has been studied with QCM-D [19,20]. The adsorbed protein layer can serve as a simplified model of a cell wall of gram-positive bacteria. The study of this single component can contribute to a deeper understanding of metal interaction. However, solely QCM-D experiments do not allow statements regarding surface structures and influences of metals to protein. Other techniques are necessary to obtain such information. One possibility for imaging bio-nanostructures and obtaining information on structural properties is the atomic force microscopy (AFM).

The objective of the presented study was to investigate the sorption of gold (Au(III) and Au(0)-NPs) to S-layer proteins, in particular Slp1 of *L. sphaericus* JG-B53. Experiments were done with suspended proteins on batch scale in a pH range of 2.0 - 5.0 using ICP-MS and with immobilized S-layers using QCM-D. Additionally, the influence of metal salt solution on the lattice stability was investigated with subsequent AFM studies. The combination of these techniques contributes to a better understanding of *in vitro* metal interaction processes as a tool for learning more about binding events on whole bacterial cells regarding specific metal affinities. This knowledge is not only crucial for the development of applicable filter materials for the recovery of metals for environmental protection and the conservation of resources [49], but also for the development of arrays of highly ordered metallic NPs for various technical applications.

Protocol

1. Microorganism and Cultivation Conditions

Note: All experiments were done under sterile conditions. *L. sphaericus* JG-B53 was obtained from a cryo-preserved culture [29,30].

1. Transfer cryo-preserved culture (1.5 ml) under the clean bench to 300 ml sterile nutrient broth (NB) media (3 g/L meat extract, 5 g/L peptone, 10 g/L NaCl). Afterwards stir the solution for at least 6 hr at 30 °C to obtain the pre-culture for cultivation.
2. Cultivate the bacteria under aerobic conditions in NB media at pH = 7.0, 30 °C in a 70 L scaled steam-in-place bioreactor. Therefore, fill the reactor with ≈ 57 L deionized water. Add and dissolve solid NB media directly in bioreactor (concentrations see above).
    1. Additionally add antifoam agent (30 µl/L NB-media) to the media to suppress foam formation during cultivation, then autoclave (122 °C, temperature holding time 30 min) the media inside the reactor facility.
3. Cool down the media and perform complete oxygen saturation. Adjust the pH to 7.0 (using 1 M H_2SO_4 and 2 M NaOH) and start the automatic inoculation of the 300 ml pre-culture. Start the data recording of cultivation parameters at the inoculation point. Log *online* parameters *e.g.,* dissolved oxygen level (dO_2), acid and base addition, and pH-values within the cultivation.

1. Monitor the bacterial growth *online* by the non-invasive turbidity measurements.

4. Perform additional sampling after every hour of cultivation and determine further parameter such as bio dry weight (BDW) and *offline* optical density (OD). Therefore, collect 20 ml cultivation broth at each sampling point under sterile conditions.
    1. Determine offline OD by photometric measurements of the adsorption at 600 nm. Use sterile filtrated NB-medium as a blank value. After reaching adsorption >0.4 dilute the cell suspension following the linearity of the Lambert-Beer law.
    2. For determination of BDW centrifuge 1 to 5 ml of bacterial suspension (depending on cell density) at 5,000 x g for 5 min at RT. Dry the obtained cell pellet at 105 °C in a heating oven up to mass stability and measure the pellet mass.

5. Take microscopic images with optical phase contrast research microscope in 400 and 1,000 fold magnification (phase contrast condenser 2 and 3 respectively) for checking of the bacterial growth and as a cross-contamination control.
6. After reaching the exponential growth phase detected by *online* dO_2 and *online* turbidity, harvest the biomass by flow-through centrifugation at 15,000 x g, 4 °C and wash the biomass twice with standard buffer (50 mM TRIS, 10 mM $MgCl_2$, 3 mM NaN_3, pH = 7.5).
   Note: The obtained biomass pellet can be stored at -18 °C until further usage for isolation.

2. S-layer Protein Isolation and Purification

Note: Purify Slp1 polymers according to an adapted method as described previously[2,19,30,32,50,51].

1. Homogenize the washed and defrosted crude biomass obtained from cultivation in standard buffer (1:1 (w/v)) to remove flagella by using a disperser (level 3, 10 min) under ice bath cooling at 4 °C.
2. Centrifuge the suspension (8,000 x g, 4 °C for 20 min) and wash the obtained pellet twice with standard buffer (1:1 (w/v)). After washing and centrifugation (8,000 x g, 4 °C for 20 min), resuspend the pellet in standard buffer (1:1 (w/v)), add DNase II and RNase (0.4 units/g biomass) to the suspension and disintegrate the cells at 1,000 bar with a high-pressure homogenizer. Afterwards centrifuge the suspension at 27,500 x g, 4 °C for 1 hr.
   Note: Control cell suspension with the research microscope. Rupture is completed when less than 2 - 3 intact cells are visible in the view field of the microscope in 400 fold magnification.
3. Wash the pellet twice with standard buffer (1:1 (w/v)) and perform the centrifugation again. Afterwards resuspend the pellet in standard buffer (2:1 (w/v)) mixed with 1% Triton X-100 and incubate it for 20 min under successive shaking (100 rpm) to solubilize lipid deposits.
4. Centrifuge the solution (27,500 x g, 4 °C for 1 hr) and wash the obtained pellet three times with standard buffer (1:1 (w/v)).
5. Incubate the pellet obtained after additional centrifugation (27,500 x g, 4 °C for 1 hr) for 6 hr in standard buffer (1:1 (w/v)) mixed with 0.2 g/L lysozyme, to hydrolyze linkages in peptidoglycan [50]. Additionally add DNase II and RNase (each 0.4 units/g biomass) to the suspension.
6. After centrifugation (45,500 x g, 4 °C, 1 hr), resuspend the upper white protein phase with a low volume of the centrifugation supernatant (<30 ml) containing protein subunits.
7. Solubilize the white suspension by mixing 1:1 with 6 M guanidine hydrochloride (6 M GuHCl, 50 mM TRIS, pH = 7.2). The solution becomes bright.
8. Perform sterile filtration (0.2 µm) of the GuHCl treated solution followed by an additional high-speed centrifugation (45,500 x g, 4 °C for 1 hr).
9. Transfer the supernatant to dialysis membrane tubes (MWCO 50,000 Dalton) and dialyzed it against recrystallization buffer (1.5 mM TRIS, 10 mM $CaCl_2$, pH = 8.0) for 48 hr.
10. Transfer the white recrystallized protein polymer solution into tubes and centrifuge at 45,500 x g, 4 °C for 1 hr. Resuspend the pellet in a low volume of ultrapure water (<30 ml).
11. Afterwards, transfer the suspension into dialysis membrane tubes and perform a dialysis against ultrapure water for 24 hr to remove buffer content.
    Note: Several changes of buffer or ultrapure water during dialysis are indispensable.
12. Lyophilize the purified Slp1 in a freeze dryer.

3. Characterization and Quantification of Slp1 for Experiments

Note: Slp1 concentration for sorption and coating experiments were quantified by UV-VIS spectrophotometry.

1. Pipette 2 µl of dissolved Slp1 sample directly onto the lower measurement pedestal of the photometer. Determine protein concentration at adsorption maximum at a wavelength of 280 nm, characteristic for proteins. Use the extinction coefficient of 0.61 to determine Slp1 concentration. Use Slp1 free solution for reference measurements.
2. Dilute the protein with the buffer (for sorption experiments in batch mode use 0.9% NaCl, pH = 6.0 and for QCM-D experiments use recrystallization buffer, pH = 8.0) to desired concentration for experiments (1 g/L and 0.2 g/L respectively).
3. Analyze Slp1 quality and molecular weight by the standard bioanalytical method sodium dodecyl sulfate polyacrylamide electrophoresis (SDS-PAGE) described by Laemmli, U. K. [52].
    1. Perform SDS-PAGE before using Slp1 within experiments and *e.g.,* after Au(0)-NP incubation using 10% polyacrylamide separation gels.
    2. For SDS-samples mix ≈10 µl of the cultivation or protein sample with sample buffer (1.97 g TRIS, 5 mg bromophenol blue, 5.8 ml glycerin, 1 g SDS, 2.5 ml β-mercaptoethanol, fill with ultrapure water to 50 ml) in a ratio of 1:1 (v/v) and pipette the mixture after 4 min incubation at 95 °C into the gel pockets.
    3. Run SDS-PAGE 30 min at a voltage of 60 V until the samples pass the collection gel and change voltage to 120 V once passing the separation gel.
    4. Remove the gels from the gel system, rinse with ultrapure water and place for 1 hr into fixation solution (10% acidic acid, 50% absolute ethanol). Afterwards, rinse the gels with ultrapure water.

5. Stain gels by using an adapted unspecific colloidal Coomassie brilliant blue method [53,54]. After destaining[72,73], take SDS-PAGE images by the gel documentation system according to manufacturer's protocol.

4. Sorption Experiments in Batch-mode and Metal Quantification

1. For batch sorption experiments prepare Au(III) stock solution from $HAuCl_4 \cdot 3\ H_2O$, dilute the metal salt and mix it with the Slp1/ NaCl solution to an initial metal concentration of 1 mM and final Slp1 concentration of 1 g/L. Perform experiments in triplets with an additional negative control without Slp1. Use a total volume of 5 ml for sorption experiments.
2. Shake the suspension continuously at RT at different pre-adjusted pH values between 2.0 to 5.0 for 24 hr (adjust pH with low concentrated HCl and NaOH solution).
3. After sorption, centrifuge the samples at 15,000 x g, 4 °C for 20 min) to separate Slp1 from supernatant.
4. Transfer the supernatant into ultrafiltration tubes (MWCO 50,000 Da) and centrifuge this at 15,000 x g, 4 °C for 20 min to remove dissolved protein monomers.
5. Determine the metal concentration in the resulting filtrate by ICP-MS [19,20] and use the results for back-calculation of sorbed metal by the Slp1 dry mass. Measuring principles, opportunities of the method and components of the used ICP-MS were described in literature [55].
    1. Prepare samples and references for ICP-MS measurements using 1% HNO_3 as matrix and rhodium as an internal standard (1 mg/ml).

5. Synthesis of Au-NP and Determination of Particle Size

Note: Citrate stabilized Au(0)-NP were synthesized according to an adapted method described previously by Mühlpfordt, H. et al. (1982) to obtain spherical particles with a diameter of 10 - 15 nm [56,57].

1. Prepare a stabilized 25 mM $HAuCl_4 \cdot 3\ H_2O$ stock for the NP formation.
2. Dilute 250 µl of this stock solution in 19.75 ml ultrapure water and incubate these at 61 °C for 15 min under successive shaking.
3. Prepare 5 ml of a second stock solution (12 mM tannic acid, 7 mM sodium citrate di-hydrate, 0.05 mM K_2CO_3) and incubate the 2nd solution separately at 61 °C for 15 min.
4. Add under constant stirring the 2nd stock solution to solution one. Stir the reaction mixture for at least 10 min at 61 °C. Afterwards cool down the solution and use it for NP coating on Slp1 lattice within QCM-D experiments.
   Note: The resulting Au(0)-NP were characterized with UV-VIS spectroscopy at the absorbance maximum of 520 nm, typically used for the detection of formed Au(0)-NPs [58]. The solution can be stored at 4 °C.
5. Analyze the size of the formed Au(0)-NP by photon correlation spectroscopy (PCS) which is also known as dynamic light scattering.
    1. For determination of NP size, transfer 1.5 ml of synthesized Au(0)-NP solution into cuvettes under dust-free conditions in a laminar flow box and analyze it with a size and zeta potential particle sizer. A detailed description of PCS and sample preparation is given in Schurtenberger, P. et al. (1993) [59] and Jain, R. et al. (2015) [60].

6. QCM-D Experiments - Slp1 Coating on Surfaces and Au-NP Adsorption onto Slp1 Lattice

Note: Measurements were carried out with a QCM-D equipped with up to four flow modules. All QCM-D experiments were performed with a constant flow rate of 125 µl/min at 25 °C. Slp1 coating and metal/NP incubation were done on SiO_2 piezoelectric AT-cut quartz sensors (Ø 14 mm) with a fundamental frequency of ≈ 5 MHz. Rinsing steps and addition of solution are marked in the figures of the representative results part. The QCM-D experiments could be described as a step by step way beginning with cleaning and surface modification of the used sensors followed by Slp1 recrystallization and later on the metal and metal NP interaction.

1. **Cleaning Procedures:**
    1. Equip the fluid cells with sensor dummies. Pump at least 20 ml (each per module) of an alkaline liquid cleansing agent (2% cleanser in ultrapure water (v/v)) through the QCM-D and tube system. Afterwards pump the fivefold volume (each per module) of ultrapure water through the system (flow rate up to 300 µl/min). Perform the cleaning according to the manufacturer's protocol.
    2. Clean the SiO_2 sensors outside the flow modules by incubation (at least 20 min) in 2% SDS solution and rinse the sensors afterwards several times with ultrapure water [61,62].
    3. Dry the crystals with filtered compressed air and place them in an ozone cleaning chamber for 20 min [63,64].
    4. Repeat the cleaning procedure twice to remove all organic contents.
    5. To remove bound metals from the sensor surface rinse the sensors with 1 M HNO_3. Afterwards, perform all rinsing steps with ultrapure water.

2. **Sensor Surface Modification by Polyelectrolytes:**
   Note: Surface modification can be done either inside (flow through procedure) or outside the flow module (LbL technique). Within these experiments the following way to modify the surfaces was used.
    1. Modify the sensors with 3 g/L of alternating PE layers of polyethylene imine (PEI, MW 25,000) and polystyrene sulfonate (PSS, MW 70,000) via dip coating using LbL technique [40,41] described previously for the special used system in the article by Suhr, M. et al. (2014) [19].
    2. Place the sensors inside the appropriate PE-solution in deep well plates and incubate these for 10 min at RT.
    3. Take the sensors out of PE-solution and rinse the sensors between every dip coating step intensively with ultrapure water.
       Note: The new surface modification consists of at least three PE layer terminating with positively charged PEI.
    4. After this external modification place the sensors inside the flow module and equilibrate the sensors by rinsing with ultrapure water before starting the experiments.

3. **Slp1 Monolayer Recrystallization:**
    1. Dissolve Slp1 in 4 M urea for converting polymers into monomers.
    2. Centrifuge the monomerized proteins at 15,000 x g, 4 °C for 1 hr to remove bigger protein agglomerates.
    3. Mix the solubilized and centrifuged Slp1 supernatant with recrystallization buffer to a final protein concentration of 0.2 g/L.
    Note: The calcium depending recrystallization of Slp1 (self-assembling) starts by addition of the recrystallization buffer. Therefore, pump the mixed solution with a flow rate of 125 µl/min to the sensors (placed inside the flow modules) immediately. The recrystallization is done after stable values of frequency and dissipation shifts were detected within QCM-D experiments.
    4. After successful protein recrystallization on top of the PE-modified sensors inside the flow modules rinse the coated sensors with recrystallization buffer or ultrapure waterintensively with a flow rate of 125 µl/min until stable values of frequency and dissipation shifts were detected.
    Note: The SiO_2 surface modification with PE for later sorption experiments onto Slp1 monolayer and AFM studies is visualized in **Figure 1**.

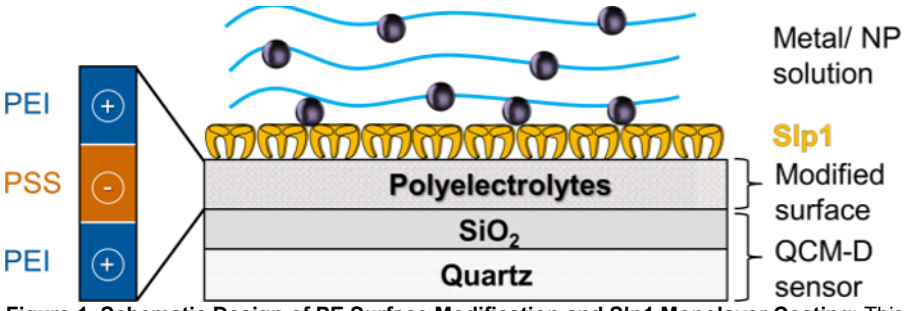

Figure 1. Schematic Design of PE Surface Modification and Slp1 Monolayer Coating; This figure has been modified from Suhr, M. et al. (2015) [19] with permission from Springer. Please click here to view a larger version of this figure.

4. **Metal and Metal NP Interaction:**
Note: The sorption with the Au metal salt solution ($HAuCl_4 \cdot 3\ H_2O$) was carried out in concentrations of 1 mM or 5 mM at pH = 6.0 in 0.9% NaCl solutions. Au-NP adsorption was done with undiluted Au-NPs in 1.6 mM tri-sodium-citrate buffer at pH ≈ 5.0.
    1. After successful Slp1 coating in the flow modules, rinse the obtained Slp1 layer intensively with 0.9% NaCl solution until stable values of frequency and dissipation shifts were detected.
    2. Pump the prepared metal solution (1 mM) and NP solution to the flow modules with a flow rate of 125 µl/min and track the mass adsorption to the Slp1 layer. Mass adsorption can be detected directly by tracking the frequency shifts referring to the Sauerbrey equation (**Equation 1**).
    3. After completing the metal and metal NP interaction, rinse the layer with metal/NP free buffer to remove weak bound or weak attached metals or nanoparticles.
    Note: An illustration of the experimental setup is shown in **Figure 2**.

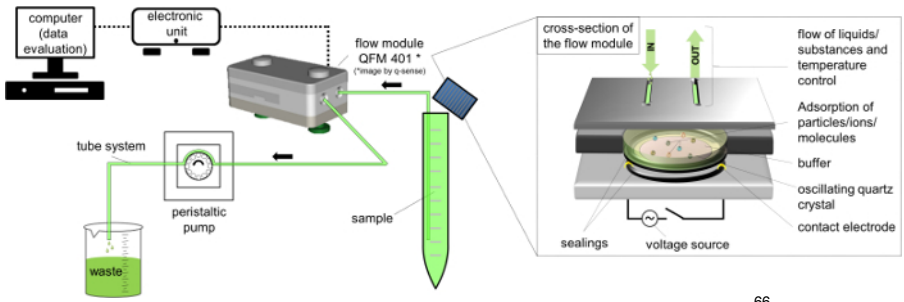

Figure 2. Schematic Design of QCM-D Setup using Flow Module QFM 401*[66]. Please click here to view a larger version of this figure.

5. **Data Recording and Evaluation**:
    1. Record the shifts in frequency in Hz (Δf_n) and dissipation (ΔD_n) within the QCM-D experiments by using QCM-D specific software.
    2. Use for evaluation of the adsorbed mass sensitivity (Δm) the Sauerbrey equation/model (**Equation 1**) [65,66] that is valid for thin and rigid films coupled without friction to the sensor surface applied to the n^{th} overtone. The term C (Sauerbrey constant) for the used 5 MHz AT cut quartz sensor is 17.7 ng · Hz^{-1} · cm^{-2}[68]. For rigid, evenly distributed, and sufficiently thin adsorbed layers use **Equation 1** as a good approximation.

$$\Delta m = -C \cdot \frac{1}{n} \cdot \Delta f_n \quad C = 17.7 \ \frac{ng}{Hz \cdot cm^2} \qquad \textbf{(Equation 1)}$$

    3. Perform additional modeling according to the Kelvin-Voigt model valid for viscoelastic molecules [68-71] with the manufacturer specific software and compare the results with that of the Sauerbrey model.
    4. For calculation of the layer thickness and mass adsorption use as important modelling parameter a layer density of the adsorbed layer of 1.35 g · cm^{-3} corresponding to values described previously for S-layer proteins [72-75]. Use the same value for the calculation of metal interaction with the proteinaceous layer.

7. AFM Measurements

1. Perform studies with fully capable AFM on an inverted optical microscope.
    1. Record AFM images in liquid using the recrystallization buffer or ultrapure water directly on the coated QCM-D sensors.
    2. Rinse the sensors with ultrapure water after QCM-D experiments and place them inside the AFM fluid cell. Therefore, use a closed fluid cell with a total volume of about 1.5 ml. Keep the temperature of the fluid cell constant at 30 °C.
    3. Use a cantilever with a resonance frequency of ≈ 25 kHz in water and a stiffness of <0.1 N/m. Adjust the scanning speed between 2.5 and 10 µm/sec.
    4. Take images in dynamic contact mode while the cantilever is excited by a piezo at its resonance frequency. Determine the distance of the cantilever to the surface by the oscillation damping [76].
    Note: Height images are shown with z-scale while z-values represent the exact topography of the surface. Amplitude (Pseudo 3D) images are shown without z-scale because amplitude z-values depend on scanning parameters and bear limited information. Analysis of images was done using three different evaluation software's [77].

Representative Results

Cultivation of Microorganisms and Slp1 Characterization

The recorded data of bacterial growth indicates the end of the exponential growth phase at around 5 hr. Previous investigations have shown that Slp1 can be isolated from this point of harvest (4.36 g/L wet biomass (≈ 1.45 g/L (BDW)) with a maximum yield [19]. Nevertheless, optimization of cultivation by using defined media components or fed-batch cultivation strategies would lead to higher biomass yields. This is inalienable for the use of high amount of biomass for industrial applications. The values from the *online* and *offline* recorded cultivation parameters are summarized in **Figure 3A**. Microscopic control (**Figure 3B**) at the time of harvest show non-sporulated cells of *L. sphaericus* JG-B53.

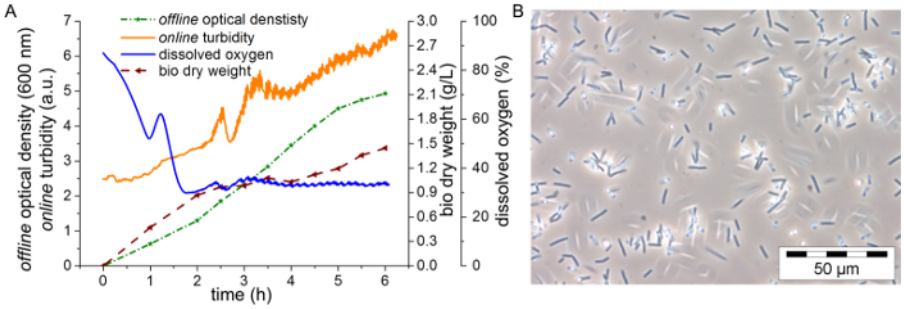

Figure 3: (**A**) *online* and *offline* measured cultivation parameters of *L. sphaericus* JG-B53 and (**B**) microscopic image of vital bacteria cells of *L. sphaericus* JG-B53 at the time of harvest in 400 fold magnification; This figure has been modified from Suhr, M. et al. (2014) [19] with permission from Springer. Please click here to view a larger version of this figure.

Also, an additionally made SDS-PAGE protein profile **(Figure 4A)** indicates the maximum amount of Slp1 at the time of 5 hr of cultivation. The protein band corresponding to Slp1 (≈ 150 kDa) is thicker, but from here on a loss in intensity was observed accompanied by an increase in proteins with lower molecular weight caused by possible protein fragmentation or segregation of other proteins. The bands of isolated and purified proteins obtained by the method mentioned above (**Figure 4B**) correspond to a molecular weight of approximately 150 kDa, which is heavier than the calculated weight based on sequencing data of Slp1 (116 kDa) [30]. This is probably due to posttranslational modifications. Other reasons for the mismatch between theoretical molecular mass and the observed molecular mass in SDS gels are possibly charge dependent artefacts in the SDS gel [30].

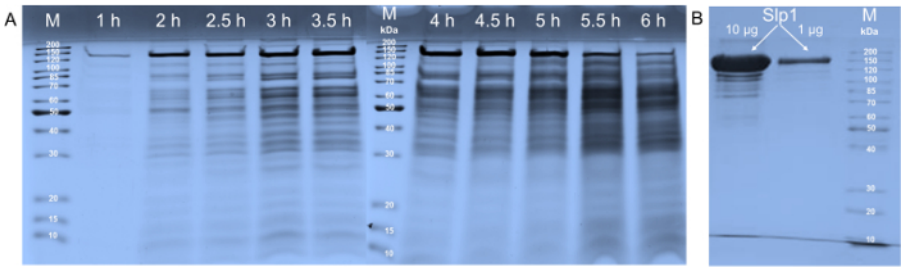

Figure 4. Protein Profiles Made by SDS-PAGE of (**A**) disintegrated bacteria cells obtained from cultivation samples and (**B**) purified Slp1 after successful isolation; This figure has been modified from Suhr, M. et al. (2014) [19] with permission from Springer. Please click here to view a larger version of this figure.

Batch-sorption Experiments and Determination of Au with ICP-MS

The maximum metal binding capacities (q_{max}) of Au(III) by suspended Slp1 are shown in **Figure 5**. The results show that Au(III) was stably bound by Slp1 during the 24 hr incubation within the investigated pH range. Results indicate q_{max} in the range of approximately 80 - 100 mg Au(III)/g Slp1. The summarized values (**Table 1**) were compared with the sorption capacity of around 75 mg Au(III)/g Slp1 reported previously by Suhr, M. et al. (2014) obtained from experiments with self-adjusting pH-values by addition of the metal salt solution (pH ≈ 4.3) [19]. To summarize, Slp1 has shown the ability to bind high amounts of initially added Au(III) proving its high binding capacities for this element.

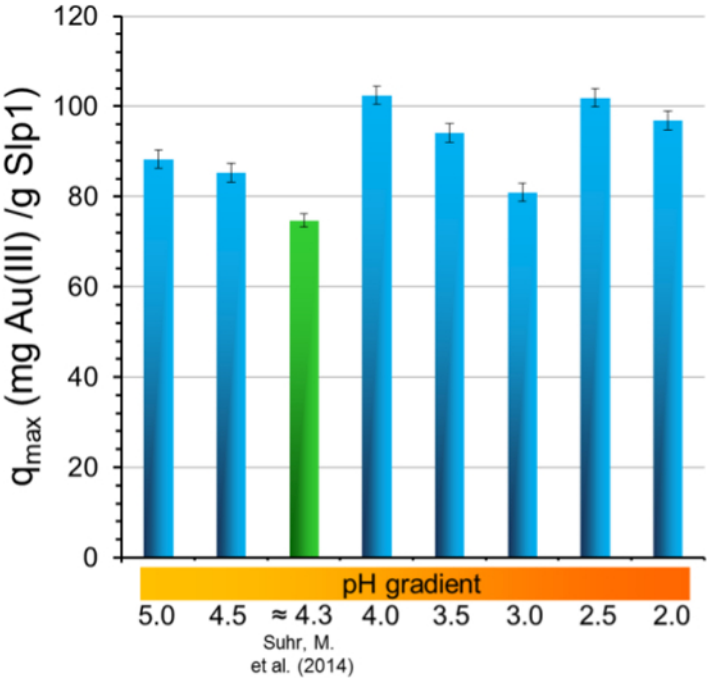

Figure 5. Diagram of Maximum Metal Binding Capacities (q_{max}) of Au(III) to Slp1 polymers within pH-adjusted experiments compared to sorption results using self-adjusted pH-values (≈ 4.3) reported by Suhr, M. et al. (2014) [19]. Please click here to view a larger version of this figure.

The calculated metal removal efficiencies (RE) within the investigated pH range were between 50 - 60% thus confirming the results made by Suhr, M. et al. (2014) where values of around 40% were achieved. In previously made experiments, strong interactions of Au(III) with the functional groups *e.g.,* carboxylic-, hydroxyl-, and amino groups, has been observed for S-layer proteins like Slp1 and for the comparative protein SlfB of *L. sphaericus* JG-A12 [1,78]. Jankowski, U. et al. (2010) detected spectroscopically a strong interaction of Au(III) mainly with carboxylic groups of SlfB that could also be deduced for Slp1 of *L. sphaericus* JG-B53 [20,79,80]. Also, intrinsic protein properties that would reduce Au(III) to Au(0) in the absence of reducing agents could be a reason for the strong interaction [79]. Furthermore, the results of this study show the tendency of a preferred binding of Slp1 at lower pH-values. On the other hand, a binding at lower pH-values could also lead to a denaturation of Slp1. Studies to the Slp1 proved a protein stability down to pH = 3.0 (unpublished results). From desorption experiments under acidic conditions, using *e.g.,* nitric acid or using complexing agents like EDTA or citrate (data not shown), verifies that gold was stably bound and could not be released from Slp1 polymers.

	Au(III) on Slp1 of L. sphaericus JG-B53							
$c_{initial}$ (mg/L)	196.97							
pH	5	4.5	≈ 4.3 [23]	4	3.5	3	2.5	2
value								
q_{max}	88.3	85.3	74.7	102.5	94.1	81	101.9	96.9
(mg Au(III) / g Slp1)								
RE	47.1	47.8	37.9	57.1	54.1	44.8	58.7	56.5
(%)								

Table 1: Maximum Metal Binding Capacities (q_{max}) and Metal Removal Efficiencies (RE) of Batch-sorption Experiments with Au(III) and Slp1 Polymers in Solution Analyzed by ICP-MS. Data compared to previously published results from Suhr, M. et al. (2014) [19].

Slp1 Monolayer Recrystallization Tracked by QCM-D

The immediate decrease in frequency (Δf_5, Δf_7, Δf_9, Δf_{11}) indicates a rapid adsorption and a high affinity of the proteins to the PE modified surface **(Figure 6A)**. Equal to the fast change in frequency, the dissipation (ΔD_5, ΔD_7, ΔD_9, ΔD_{11}) also increases immediately. This fact indicates an adsorption of viscoelastic molecules to the surface because of fast damping resulting in increasing dissipation values. The maximum frequency shift is achieved after 5 min with a value of ≈ 95 Hz and ΔD of 4.2. At a later stage only rearrangements of recrystallized Slp1 occur. Slp1 adsorption was thusly carried out for over 60 min to ensure the formation of an almost fully covered surface and regularly ordered protein lattice. The experiment shows that the positively charged PE layer is inalienable for achieving stable coatings, negative ending modification leads to a weak adsorption and longer coating kinetics (data not shown) [38]. Weakly attached proteins and agglomerates were removed by rinsing with Slp1-free recrystallization buffer. The small changes of Δf_n confirm the low protein desorption and stable adsorption of Slp1. Despite this the dissipation drops down to ≈ 2.8 indicating that bigger elastic molecules are removed.

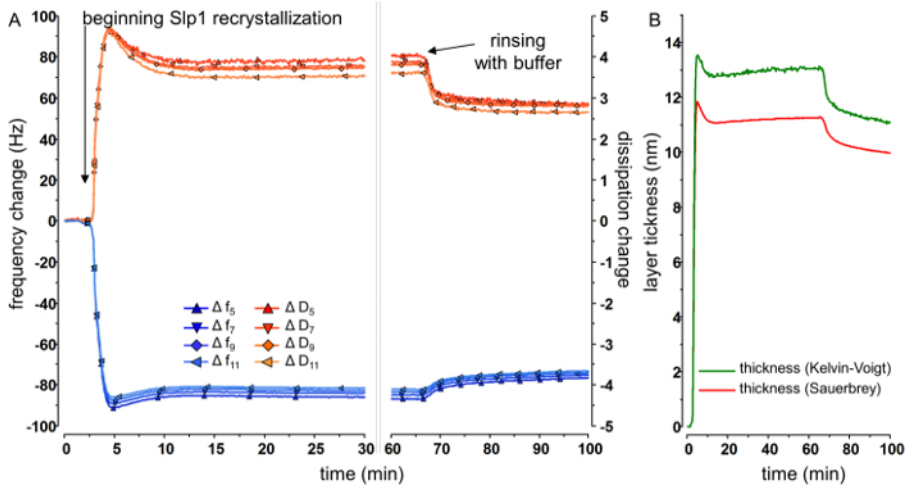

Figure 6. Recrystallization of Slp1 on Modified SiO_2 Sensors Analyzed by QCM-D; (**A**) in Δf/ΔD plot and (**B**) surface thickness profile; This figure has been modified from Suhr, M. et al. (2014) [19] with permission from Springer and Suhr, M. (2015) [20]. Please click here to view a larger version of this figure.

The surface profile calculated by using the previous mentioned models show a Slp1 monolayer thickness of ≈ 11.2 nm (Kelvin-Voigt model for elastic films) and of 10.0 nm (Sauerbrey model for rigid layer) **(Figure 6B).** These values are lower than those reported by Suhr, M. et al. (2014). The differences can be explained by a different used value of protein layer density within the modelling. The current values should be closer to realities of layer thickness of S-layer proteins on the cell surface of living cells of *L. sphaericus* JG-B53 [31,42]. This modelling demonstrates that the Sauerbrey relation is inappropriate for acoustical thin proteinaceous layer, because of a propagation of the shear acoustic wave in viscoelastic liquid films [81,82] that results in an underestimation of the adsorbed Slp1 mass and thickness. This can be explained by the elastic properties of S-layer proteins and its coupling of water molecules during the adsorption process. The interaction of water with proteins can be easily described by formation of hydration shells, viscous drag or entrapment in cavities in the adsorbed layer [83]. This effects a higher layer thickness measured by the Kelvin-Voigt model and can also clarify the differences in the layer thickness obtained by the two different models. In previous AFM studies, layer thicknesses of Slp1 lattices of around 8-12 nm were measured. By calculating the mass adsorption of Slp1, instead of layer thickness, a total Δm of 1506.6 ng · cm^{-2} (Kelvin-Voigt model) was calculated. The data of mass adsorption on surfaces are summed up in **Table 2** and show a high mass adsorption by using the values of the Kelvin-Voigt model.

	m_{max}	**Δm_{max}**	**thickness**	**thickness**
	(ng/cm^2)	**(ng/cm^2)**	**(nm)**	**(nm)**
	(Kelvin-Voigt)	**(Sauerbrey)**	**(Kelvin-Voigt)**	**(Sauerbrey)**
Slp1 after coating and rinsing	1,505.6	1,351.6	11.2	10

Table 2: Adsorbed Mass of Slp1 on Modified Polyelectrolyte SiO_2 Crystals Analyzed by QCM-D after Rinsing with Recrystallization Buffer (pH = 8.0) and Calculated Layer Thickness.

QCM-D as Tool for Detection of Metal and Metal NP Interaction with Proteinaceous Slp1 Monolayer

The interaction of recrystallized Slp1 monolayer with 1 mM and 5 mM dissolved Au(III) was investigated. The results of total adsorbed mass obtained from calculations and modeling of the recorded data of changes in frequency and dissipation are summarized in **Table 3**. The QCM-D studies of Au(III) interaction with the monolayers provide a deeper understanding of the metal-biomolecule interaction. For the first time, the binding capacity, sorption kinetics, and how the metal influences the protein stability were studied in a nano-range. After the addition of the metal salt solution to the Slp1 monolayer the frequency decreased within the first 5 min indicating a fast mass adsorption. Nevertheless, the adsorption of Au was not completed after 60 min as described for other metals like Pd(II) in previous studies [19]. The mass increase occurs up to 18 hr. After this time, rinsing steps were performed with metal free buffer showing that the adsorbed metal is almost stably bound to the recrystallized Slp1 layer. Finally, a total metal absorption of 955.0 ± 2.7 ng · cm^{-2} (Kelvin-Voigt model) was obtained in case of the 1 mM Au(III) solution and 4,534.4 ± 5.5 ng · cm^{-2} (Kelvin-Voigt model) in case of 5 mM Au(III). The higher values obtained by 5 mM Au(III) solutions can be explained by intrinsic reduction properties of Slp1 where smallest metallic Au(0)-NP were formed from this solution. These reducing properties of Slp1 have been already reported in previous studies for Pd(II) and Au(III) [32,33,79,84]. The data also showed that the interaction with the gold solution does not lead to a destabilization of the protein layers. This indicates the specific and stable binding of Au(III) to Slp1, which has been also confirmed by ICP-MS measurements using protein polymers.

The formation of Au(0)-NP during the synthesis could be visualized by color change from the starting yellow solution to a reddish one. This color change is caused by the excitation of the surface plasmon oscillations of metallic nanoparticles and proves the formation of Au(0)-NPs [1,78]. Furthermore smaller NPs could be synthesized by the variation of the concentration of the reducing agent (higher tannic acid concentration) [85] visible in a different coloring of solution and verified by results of PCS measurements (data not shown). On the other hand, increasing tannic acid concentration leads to a loss of NP stability and NPs tend to agglomerate [20]. As proof of principle, pre-synthesized Au(0)-NPs (size distribution of 10 - 18 nm measured by PCS seen in **Figure 7A**) were incubated with suspended Slp1 for 48 hr and analyzed by SDS-PAGE. The protein profile shown in **Figure 7B** verifies the conclusion drawn from QCM-D data, that Au(0)-NPs do not disturb the Slp1 structure. The observed protein bands at 150 kDa prove the presence of intact Slp1.

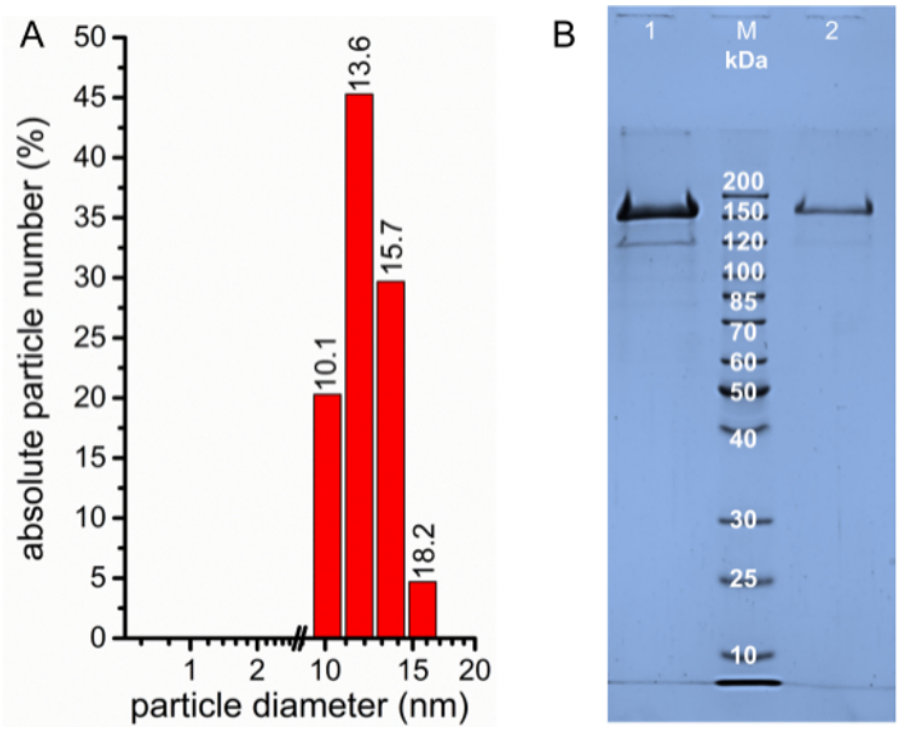

Figure 7. (**A**) Number weighted size distribution of pre-synthesized Au(0)-NPs measured by PCS and (**B**) SDS-PAGE protein profile of Slp1; lane 1: 2 µg Slp1 before Au(0)-NPs interaction and lane 2: 1 µg Slp1 polymers in suspension after 48 hr incubation with pre-synthesized Au(0)-NPs. Please click here to view a larger version of this figure.

After the NP-synthesis and characterization, QCM-D experiments were carried out. The adsorption of pre-synthesized metallic Au(0)-NPs is exemplarily shown for QCM-D experiments in Δf/ΔD plots (**Figure 8A**) and as thickness and mass profiles (**Figure 8B**).

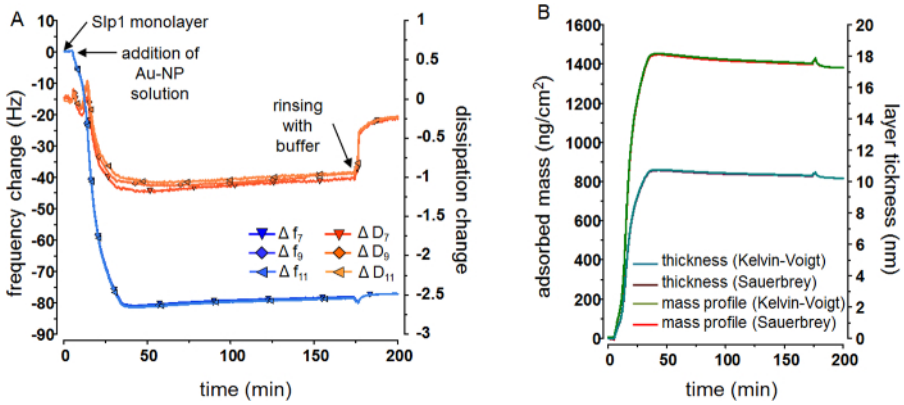

Figure 8. Adsorption of Pre-synthesized Au(0)-NPs onto Recrystallized Slp1 Lattice Analyzed by QCM-D, (**A**) in Δf/ΔD plot and (**B**) layer surface and mass profile. Please click here to view a larger version of this figure.

It could be confirmed that QCM-D can be used to detect the adsorption of the 10 - 18 nm spherical Au(0)-NPs. After addition of the undiluted Au-NP solution ($A_{520\ nm}$ = 1) obtained by the described synthesis, the frequency decreases, which is a direct indicator of mass adsorption described by the prediction of the Sauerbrey equation (**Equation 1**). The adsorption of Au(0)-NPs was almost completed within less than 60 min. After this time no more NPs were deposited on the top of the Slp1 lattice, so it can be assumed that all reactive sites or pores were occupied by Au(0)-NPs. The shown decrease in dissipation can be affiliated to the stiffening of Slp1 lattice cause by the NP interaction. The values of total mass adsorption are summed up in **Table 3**. Even intensive rinsing with the NP-free citrate buffer leads neither to a desorption of NPs nor to a detachment of the Slp1 monolayer. Therefore, a stable and strong interaction can be predicted for the Au(0)-NP interaction in the same respect as with Au(III).

Metal	**c_{metal}**	**Δm_{max} (ng/cm²) (Kelvin-Voigt)**	**Δm_{max} (ng/cm²) (Sauerbrey)**	**thickness (nm) (Kelvin-Voigt)**	**thickness (nm) (Sauerbrey)**
Au(III)	1 mM	955	932.6	---	---
	5 mM	4,534.4	4,687.9	---	---
Au(0)-NPs	---	1,382.9	1,382.7	10.2	10.2

Table 3: Adsorbed Mass on Recrystallized Slp1 Lattice after Au(III) Interaction (pH = 6.0) and Au-NP Adsorption (pH = 4.7) Analyzed by QCM-D and Calculation of Layer Thickness after Au(0)-NP Coating. Data compared to previously published results from Suhr, M. et al. (2014) [19].

AFM for Visualization of Nanometer Scaled Structures

Subsequent AFM studies after QCM-D experiments were performed to obtain structural information of Slp1 self-assemblies before and after their interaction with metals and NPs. This is necessary to correlate the mass adsorption detected during the QCM-D experiments with the completeness of protein coatings and the protein lattice structures allowing statements about protein layer stability. In **Figure 9**, the protein lattice of Slp1 recrystallized on PE modified sensors is shown with its typical square lattice (*p4*) as amplitude images. The lattice constant could be determined as 13 - 14 nm, which is comparable to results of previous experiments [30]. The layer thickness of 10 nm ± 2.0 nm measured by AFM verified the predicted layer thickness of the QCM-D measurements of ≈ 11.2 nm (Kelvin-Voigt modelling). The small difference in the surface height can be explained by the fact that the calculated QCM-D fit considers the whole sensor area while the high resolution AFM study only shows a partial area. Given this, protein agglomerates that were attached to the sensor surface were included in the calculation of the adsorbed mass respectively to the layer thickness and led to a higher layer thickness than determined by AFM.

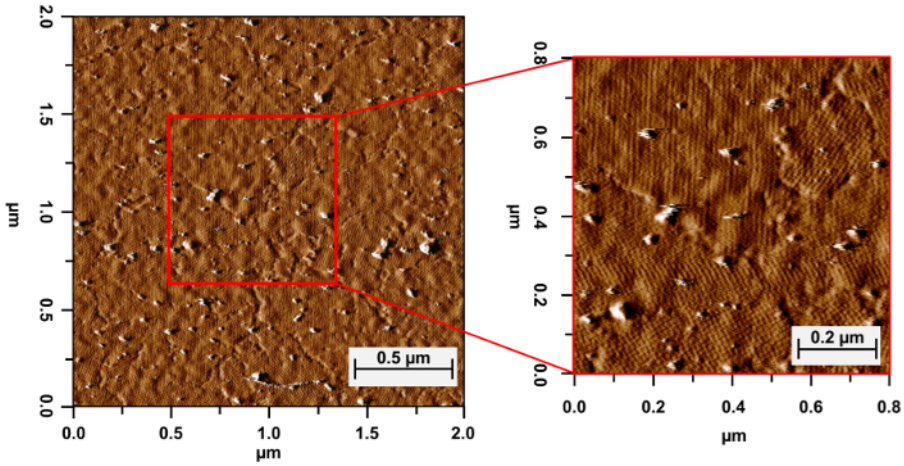

Figure 9. AFM Amplitude Image of Recrystallized Slp1 Lattice of *L. sphaericus* JG-B53 on QCM-D Crystals Directly after Coating and Rinsing with Buffer and Magnification of Marked Region; This figure has been modified from Suhr, M. et al. (2014) [19] with permission from Springer. Please click here to view a larger version of this figure.

Subsequent to Au(III) and Au(0)-NP interaction with Slp1 and measurements performed with QCM-D, the sensor surfaces were investigated by AFM. **Figure 10** shows the intact Slp1 lattice after incubation with Au(III) solution. It can be shown that after the incubation the protein lattice remained completely intact. This confirms the results from the QCM-D experiments that predicted the stability of the coating. In **Figure 11A and B** the adsorbed pre-synthesized Au(0)-NPs (size varies from 10 - 18 nm determined by PCS) on the Slp1 lattice are shown. Due to the particle size, the Au(0)-NPs are adsorbed in the Slp1 pores and do not follow the *p4*-symmetry of Slp1. Au(0)-NPs are statistical distributed on protein lattice. By measuring the particle sizes in AFM height images (data not shown) the size of the NPs is in the range of 16 - 23 nm and even smaller, namely in the range of approximately 10 nm [19,20]. This verifies the determined NP size measured previously by PCS (seen in **Figure 8**).

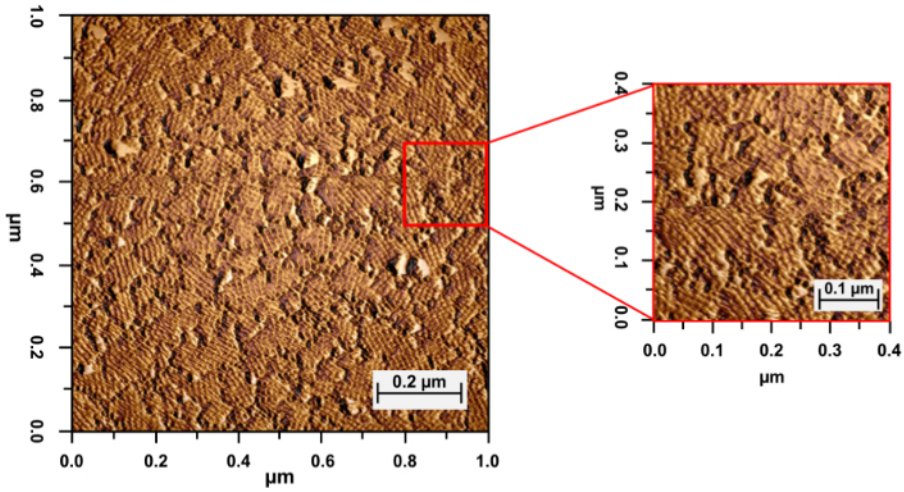

Figure 10. AFM Amplitude Image of Recrystallized and Intact Slp1 Lattice on QCM-D Sensor Crystals after Incubation of 5 mM Au(III) Solution and Magnification of Marked Region; This figure has been modified from Suhr, M. et al. (2014) [19] with permission from Springer and Suhr, M. (2015) [20]. Please click here to view a larger version of this figure.

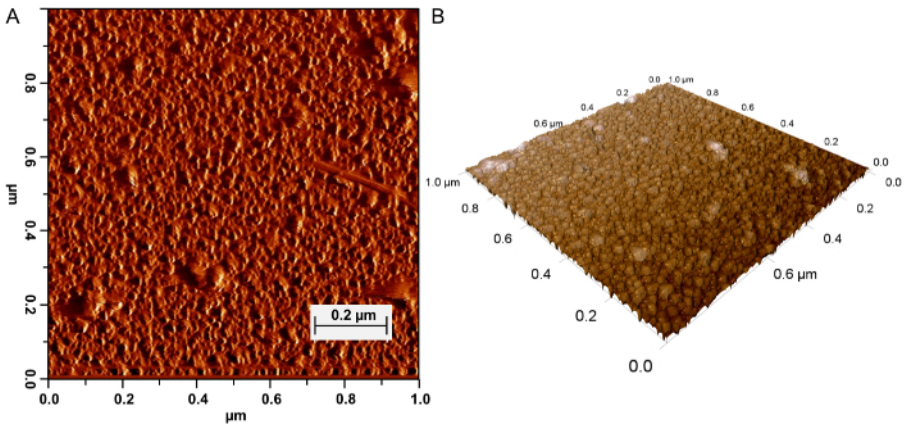

Figure 11. (**A**) AFM amplitude image of adsorbed Au(0)-NPs on recrystallized Slp1 lattice on QCM-D sensor crystals (left) and (**B**) 3D reconstructed surface profile (right); This figure has been modified from Suhr, M. (2015) [20] with permission from Springer and Raff, J. et al. (2016) [Raff, J. et al. S-layer based nanocomposites for industrial applications in Protein-based Engineered Nanostructures. (eds Tijana Z. Grove & Aitziber L. Cortajarena) (Springer, 2016 (submitted))].

Please click here to view a larger version of this figure.

Discussion

In this work studied the binding of Au to S-layer proteins was investigated using a combination of different analytical methods. In particular, the binding of Au is very attractive not only for the recovery of Au from mining waters or process solutions, but also for the construction of materials, *e.g.,* sensory surfaces. For studies of the Au interaction (Au(III) and Au(0)-NPs) with suspended and recrystallized monolayer of Slp1, the protein had to be isolated. Therefore, this study has shown the successful cultivation of the gram-positive bacterial strain *L. sphaericus* JG-B53 and the isolation of the surface layer protein Slp1. Nevertheless, the cultivation and protein isolation remain challenging and should be optimized. A large scale production of biomass and S-layer proteins is a precondition for an industrial application of both, *e.g.,* for the production of metal selective filter materials. Their application potential is undoubtedly high for the removal of toxic metals or the recovery of valuable metals dissolved in process water, waste water, or drainage water. Furthermore, the application potential for S-layers is even larger considering their additional potential in other bio-inspired materials, such as biosensors and catalysts.

The batch-sorption experiments of suspended Slp1 polymers indicated a high and stable binding of Au(III) within the investigated pH-range from 2.0 to 5.0. Thereby, metal removal efficiencies of up to 60% could be reached. This remarkable binding behavior can be explained by a strong interaction of Au(III) with Slp1 probably induced through interaction of carboxylic groups and nitrogen bearing groups present on the surface of the protein. This arguments could be strengthen by FTIR and EXAFS investigation of the similar strain *L. sphaericus* JG-A12 [32,79]. Also, intrinsic reducing properties of Slp1 can explain the high RE of Au(III) by reducing it to nanoparticular Au(0). It can be assumed that S-layer, as first interface of bacteria to the environment, should be mainly involved in metal binding. Within the investigated pH range, the highest metal binding capacity with 102.5 mg Au(III)/g Slp1 was achieved at pH 4.0. This binding capacity is higher than reported for other bio-components, *e.g.,* for isolated cell wall of *Bacillus subtilis* (71.5 mg Au(III)/g) [86] or for biomass of *Chlorella vulgaris* (98.5 mg Au(III)/g) [8].

ICP-MS used for determination of the bound metal by Slp1 polymers is very sensitive method and enables the detection of smallest amounts of gold in this study. ICP-MS offers many benefits for performing trace metal determinations, *e.g.,* easy handling system and low detection limits; in case of gold down to 0.1 - 1 ppt. This makes this method a versatile tool for investigating biosorptive processes in low concentration ranges. However, the results in this investigation were gained with suspended S-layer polymers and cannot be easily transferred to S-layer lattices recrystallized on surfaces, and therefore show the limitation of ICP-MS. For example, no direct relation of isolated protein polymers could be made to those S-layer structures on vital bacteria cells. In addition, the ICP-MS measurements do not allow the determination of the kinetic of metal sorption. Therefore, it is necessary to find methods more suitable for the investigation of the metal binding by thin immobilized protein films.

In the present study, QCM-D analyses were applied to detect the *in situ* formation of S-layer lattices on surfaces as well as the deposition of Au on the proteins. Therefore, QCM-D is a robust and reproducible method for the recognition of molecule adsorption and interaction processes . Additionally QCM-D is a relatively simple, cost-effective, and nonhazardous method to monitor such processes *online*. The method has the advantage to detect mass change with a maximum mass sensitivity in liquids of ≈ 0.5 ng · cm^{-2}. This enables the possibility to detect even weak interaction, *e.g.,* of protein with dissolved metals or to measure adsorptions in low concentration ranges. The disadvantage of QCM-D is that this is not a structure imaging method that allows the visualization of *e.g.,* protein lattices. Therefore, other techniques are needed.

The QCM-D analyses in this study were followed by AFM imaging. The combination of these methods allowed the study of the sorption kinetics and consequences of Au sorption for the coating, thus proving that they are versatile tools for investigating metal interaction of thin proteinaceous films. Further, it was shown that a reliable recrystallization of the S-layer proteins on technical supports is essential for subsequent protein interaction studies. Therefore, modifications of the surfaces using adhesion promotors are of interest. The described implementation of polyelectrolytes (ending with positively charged PEs) as intermediate layer between SiO_2 surfaces and protein layer lead to an improved method for a fast protein coating. The positive effect of a positively charge polyelectrolyte layer has been described previously for *e.g.,* immobilization of vital bacteria cells of *L. sphaericus* JG-B53 [31]. The implementation of the presented PE-layers are the most important and critical step for the later successful and reproducible recrystallization of S-layer proteins.

It could be demonstrated that for the investigation of thin layers of Slp1, QCM-D is a good method to show the mass adsorption respective to the protein recrystallization as monolayer films in real time. This could also be observed previously for the reassembly of the S-layer protein

SbpA of *L. sphaericus* CCM2177 [47]. By using subsequent high-resolution AFM analyses changes of the lattice structure of the protein self-assemblies can be visualized. AFM measurements revealed the *p4* symmetry of Slp1 and confirm the modelled layer thickness of Slp1 of about 10 nm. Also, the direct interaction of dissolved metal ions with the protein layer could be monitored by QCM-D proving good binding of Au(III) by the underlying protein layer. The probable formation of the smallest Au(0)-NPs from Au(III) solution inside protein pores caused by intrinsic reducing properties of the Slp1 lattice within QCM-D measurements could not been detected by subsequent AFM measurements. This could be related to the resolution limit of AFM and the experimental set up in this study. This shows the limitation of this technique and the necessity of high resolution imaging for biomolecules in the sub nanometer scale. However, a high stability of the recrystallized Slp1 layer could be deduced from the obtained QCM-results and was confirmed by AFM investigation.

In conclusion, it could be shown that Slp1 polymers have high metal binding capacities for gold within the investigated pH-range. Furthermore, the investigation reveals that the Slp1 lattice is a good matrix metal ion binding and for the immobilization of metallic nanoparticles. It could be shown that each method used in this article has the possibility to detect even small metal interactions, or in case of AFM can visualize structures in the nanoscale range. Although, it is only by the combination of these shown methods, that has allowed to improve the knowledge and understanding of the investigated proteins on a molecular level.

Mainly, QCM-D and AFM are the preferred methods of choice for future investigation of protein monolayer adsorption and their interaction with metals and functional molecules. By combining these two methods, the detection of S-layer protein adsorption processes and surface imaging provides an insight into molecular processes that may be able to be transferred to enhance the knowledge of living bacteria and the interaction with their environment. This study showed an excerpt of possible methods helpful for understanding protein and metal interaction. Other helpful techniques that could enhance the knowledge of such processes in detail ranging from diverse spectrometric and chromatographic methods to spectroscopic investigation of biomolecules and should be included in future studies.

Disclosures

The authors have nothing to disclose.

Acknowledgements

The present work was partially funded by the IGF-project "S-Sieve" (490 ZBG/1) funded by the BMWi and the BMBF-project "Aptasens" (BMBF/DLR 01RB0805A). Special thanks to Tobias J. Günther for his valuable help during AFM studies and to Erik V. Johnstone for reading the manuscript as a native English speaker. Further, the author of this paper would like to thank Aline Ritter and Sabrina Gurlit (from Institute for Resource Ecology for assistance in ICP-MS measurements), Manja Vogel, Nancy Unger, Karen E. Viacava and the group biotechnology of the Helmholtz-Institute Freiberg for Resource Technology.

References

1. Merroun, M. L., Rossberg, A., Hennig, C., Scheinost, A. C., & Selenska-Pobell, S. Spectroscopic characterization of gold nanoparticles formed by cells and S-layer protein of *Bacillus sphaericus.* JG-A12. *Mater. Sci. Eng. C.* **27** (1), 188-192 (2007).
2. Raff, J., Soltmann, U., Matys, S., Selenska-Pobell, S.; Bottcher, H., Pompe, W. Biosorption of uranium and copper by biocers. *Chem. Mat.* **15** (1), 240-244 (2003).
3. Sleytr, U. B., Schuster, B., Egelseer, E.-M., & Pum, D. S-Layers: Principles and Applications. *FEMS Microbiol. Rev.*, (2014).
4. Pollmann, K., Raff, J., Merroun, M., Fahmy, K., & Selenska-Pobell, S. Metal binding by bacteria from uranium mining waste piles and its technological applications. *Biotechnol. Adv.* **24** (1), 58-68 (2006).
5. Raff, J., & Selenska-Pobell, S. Toxic avengers. *Nucl. Eng. Int.* **51** 34-36 (2006).
6. Tsuruta, T. Biosorption and recycling of gold using various microorganisms. *J. Gen. Appl. Microbiol.* **50** (4), 221-228 (2004).
7. Sathishkumar, M., Mahadevan, A., Vijayaraghavan, K., Pavagadhi, S., & Balasubramanian, R. Green Recovery of Gold through Biosorption, Biocrystallization, and Pyro-Crystallization. *Ind. Eng. Chem. Res.* **49** (16), 7129-7135 (2010).
8. Das, N. Recovery of precious metals through biosorption - A review. *Hydrometallurgy.* **103** (1-4), 180-189 (2010).
9. Volesky, B. Biosorption and me. *Water Res.* **41** (18), 4017-4029 (2007).
10. Vilar, V. J. P., Botelho, C. M. S., & Boaventura, R. A. R. Environmental Friendly Technologies for Wastewater Treatment: Biosorption of Heavy Metals Using Low Cost Materials and Solar Photocatalysis in *Security of Industrial Water Supply and Management.NATO Science for Peace and Security Series C-Environmental Security.* (eds A. T. Atimtay & S. K. Sikdar) 159-173 Springer, (2010).
11. Lovley, D. R., & Lloyd, J. R. Microbes with a mettle for bioremediation. *Nat. Biotechnol.* **18** (6), 600-601 (2000).
12. Schiewer, S., & Volesky, B. in *Environmental Microbe-Metal Interactions.* (ed D.R. Lovley) 329-362 ASM Press, Washington, (2000).
13. Raff, J., Berger, S., Selenska-Pobell, S. Uranium binding by S-layer carrying isolates of the genus *Bacillus.* Annual Report Forschungszentrum Rossendorf - Institute of Radiochemistry, Dresden, (2006).
14. Srinath, T., Verma, T., Ramteke, P. W., & Garg, S. K. Chromium (VI) biosorption and bioaccumulation by chromate resistant bacteria. *Chemosphere.* **48** (4), 427-435 (2002).
15. Godlewska-Zylkiewicz, B. Biosorption of platinum and palladium for their separation/preconcentration prior to graphite furnace atomic absorption spectrometric determination. *Spectroc. Acta Pt. B-Atom. Spectr.* **58** (8), 1531-1540 (2003).
16. Hosea, M. *et al.* Accumulation of elemental gold on the alga *Chlorella-vulgaris. Inorg. Chim. A-Bioinor.* **123** (3), 161-165 (1986).
17. Vogel, M. *et al.* Biosorption of U(VI) by the green algae *Chlorella vulgaris.* in dependence of pH value and cell activity. *Sci. Total Environ.* **409** (2), 384-395 (2010).
18. Creamer, N., Baxter-Plant, V., Henderson, J., Potter, M., & Macaskie, L. Palladium and gold removal and recovery from precious metal solutions and electronic scrap leachates by *Desulfovibrio desulfuricans. Biotechnol Lett.* **28** (18), 1475-1484 (2006).
19. Suhr, M. *et al.* Investigation of metal sorption behavior of Slp1 from *Lysinibacillus sphaericus.* JG-B53 - A combined study using QCM-D, ICP-MS and AFM. *Biometals.* **27** (6), 1337-1349 (2014).

20. Suhr, M. PhD thesis, *Isolierung und Charakterisierung von Zellwandkomponenten der gram-positiven Bakterienstämme Lysinibacillus sphaericus JG-A12 und JG-B53 und deren Wechselwirkungen mit ausgewählten relevanten Metallen und Metalloiden.* PhD thesis, Technische Universität Dresden, (2015).
21. Spain, A., & Alm, E. Implications of Microbial Heavy Metal Tolerance in the Environment. *Reviews in Undergraduate Research.* Vol. **2** 1-6 Rice University Houston (USA), (2003).
22. Ledin, M. Accumulation of metals by microorganisms - processes and importance for soil systems. *Earth-Sci. Rev.* **51** (1-4), 1-31 (2000).
23. Maruyama, T. *et al.* Proteins and Protein-Rich Biomass as Environmentally Friendly Adsorbents Selective for Precious Metal Ions. *Environ. Sci. Technol.* **41** (4), 1359-1364 (2007).
24. Sara, M., & Sleytr, U. B. S-layer proteins. *J. Bacteriol.* **182** (4), 859-868 (2000).
25. Baranova, E. *et al.* SbsB structure and lattice reconstruction unveil Ca2+ triggered S-layer assembly. *Nature.* **487** (7405), 119-122 (2012).
26. Teixeira, L. M. *et al.* Entropically Driven Self-Assembly of Lysinibacillus sphaericus S-Layer Proteins Analyzed Under Various Environmental Conditions. *Macromol. Biosci.* **10** (2), 147-155 (2010).
27. Ahmed, I., Yokota, A., Yamazoe, A., & Fujiwara, T. Proposal of Lysinibacillus boronitolerans gen. nov. sp. nov., and transfer of Bacillus fusiformis to Lysinibacillus fusiformis comb. nov. and Bacillus sphaericus to Lysinibacillus sphaericus comb. nov. *Int. J. Syst. Evol. Microbiol.* **57** (5), 1117-1125 (2007).
28. Panak, P. *et al.* Bacteria from uranium mining waste pile: interactions with U(VI). *J. Alloy. Compd.* **271**, 262-266 (1998).
29. Selenska-Pobell, S., Kampf, G., Flemming, K., Radeva, G., & Satchanska, G. Bacterial diversity in soil samples from two uranium waste piles as determined by rep-APD, RISA and 16S rDNA retrieval. *Antonie Van Leeuwenhoek.* **79** (2), 149-161 (2001).
30. Lederer, F. L. *et al.* Identification of multiple putative S-layer genes partly expressed by *Lysinibacillus sphaericus.* JG-B53. *Microbiology.* **159** (Pt 6), 1097-1108 (2013).
31. Günther, T. J., Suhr, M., Raff, J., & Pollmann, K. Immobilization of microorganisms for AFM studies in liquids. *RSC Advances.* **4**, 51156-51164 (2014).
32. Fahmy, K. *et al.* Secondary Structure and Pd(II) Coordination in S-Layer Proteins from *Bacillus sphaericus.* Studied by Infrared and X-Ray Absorption Spectroscopy. *Biophys. J.* **91** (3), 996-1007 (2006).
33. Pollmann, K., Merroun, M., Raff, J., Hennig, C., & Selenska-Pobell, S. Manufacturing and characterization of Pd nanoparticles formed on immobilized bacterial cells. *Lett. Appl. Microbiol.* **43** (1), 39-45 (2006).
34. Corti, C., & Holliday, R. *Gold: science and applications.* first edn, CRC Press - Taylor&Francis Group, (2010).
35. Daniel, M.-C., & Astruc, D. Gold nanoparticles: assembly, supramolecular chemistry, quantum-size-related properties, and applications toward biology, catalysis, and nanotechnology. *Chem. Rev.* **104** (1), 293-346 (2004).
36. Tang, J. *et al.* Fabrication of Highly Ordered Gold Nanoparticle Arrays Templated by Crystalline Lattices of Bacterial S-Layer Protein. *Chem. Phys. Chem.* **9** (16), 2317-2320 (2008).
37. Haruta, M. Size- and support-dependency in the catalysis of gold. *Catal. Today.* **36** (1), 153-166 (1997).
38. Habibi, N. *et al.* Nanoengineered polymeric S-layers based capsules with targeting activity. *Colloids and surfaces. B, Biointerfaces.* **88** (1), 366-372 (2011).
39. Toca-Herrera, J. L. *et al.* Recrystallization of Bacterial S-Layers on Flat Polyelectrolyte Surfaces and Hollow Polyelectrolyte Capsules. *Small.* **1** (3), 339-348 (2005).
40. Decher, G., Lehr, B., Lowack, K., Lvov, Y., & Schmitt, J. New nanocomposite films for biosensors - Layer-by-Layer adsorbed films of polyelectrolytes, proteins or DNA. *Biosens. Bioelectron.* **9** (9-10), 677-684 (1994).
41. Decher, G., & Schmitt, J. *Fine-tuning of the film thickness of ultrathin multilayer films composed of consecutively alternating layers of anionic and cationic polyelectrolytes.* Vol. **89** Dr Dietrich Steinkopff Verlag, (1992).
42. Günther, T. J. PhD thesis, *S-Layer als Technologieplattform - Selbstorganisierende Proteine zur Herstellung funktionaler Beschichtungen.* PhD thesis, Technische Universität Dresden, (2015).
43. Delcea, M. *et al.* Thermal stability, mechanical properties and water content of bacterial protein layers recrystallized on polyelectrolyte multilayers. *Soft Matter.* **4** (7), 1414-1421 (2008).
44. Roach, P., Farrar, D., & Perry, C. C. Interpretation of Protein Adsorption: Surface-Induced Conformational Changes. *J. Am. Chem. Soc.* **127** (22), 8168-8173 (2005).
45. Zeng, R., Zhang, Y., Tu, M., & Zhou, C. R. Protein Adsorption Behaviors on PLLA Surface Studied by Quartz Crystal Microbalance with Dissipation Monitoring (QCM-D) in *Materials Research, Pts 1 and 2.* Vol. **610-613** *Materials Science Forum.* (eds Z. W. Gu *et al.*) 1219-1223 Trans Tech Publications Ltd, (2009).
46. Bonroy, K. *et al.* Realization and Characterization of Porous Gold for Increased Protein Coverage on Acoustic Sensors. *Anal. Chem.* **76** (15), 4299-4306 (2004).
47. Pum, D., Toca-Herrera, J. L., & Sleytr, U. B. S-layer protein self-assembly. *Int. J. Mol. Sci.* **14** (2), 2484-2501 (2013).
48. Weinert, U. *et al.* S-layer proteins as an immobilization matrix for aptamers on different sensor surfaces. *Eng. Life Sci.*, (2015).
49. Umeda, H. *et al.* Recovery and Concentration of Precious Metals from Strong Acidic Wastewater. *Mater. Trans.* **52** (7), 1462-1470 10.2320/matertrans.2010432 (2011).
50. Engelhardt, H., Saxton, W. O., & Baumeister, W. 3-Dimensional structure of the tetragonal surface-layer of *Sporosarcina-urea. J. Bacteriol.* **168** (1), 309-317 (1986).
51. Sprott, G. D., Koval, S.F., Schnaitman, C.A. *Methods for general and molecular bacteriology.* 72-103 American Society for Microbiology, (1994).
52. Laemmli, U. K. Cleavage of Structural Proteins during Assembly of Head Bacteriophage T4. *Nature.* **227** (5259), 680-5 (1970).
53. Stoscheck, C. [6] Quantitation of protein in *Methods in Enzymology.* Vol. **182** (eds Murray P. Deutscher) 50-68 Academic Press, (1990).
54. Sleytr, U. B., Messner, P., & Pum, D. Analysis of Crystalline Bacterial Surface-Layers by Freeze-Etching, Metal Shadowing, Negative Staining and Ultra-Thin Sectioning. *Method Microbiol.* **20**, 29-60 (1988).
55. ICP Mass Spectrometry - The 30-Min Guide to ICP-MS. Technical note. *PerkinElmer, Inc., USA,* (2001).
56. Mühlpfordt, H. The preparation of colloidal Gold Nanoparticles using tannic-acid as an additional reducing agent. *Experientia.* **38** (9), 1127-1128 (1982).
57. Hayat, M. A. *Colloidal Gold - Principles, Methods and Applications.* Academic Press, INC, (1989).
58. Amendola, V., & Meneghetti, M. Size Evaluation of Gold Nanoparticles by UV−vis Spectroscopy. *The Journal of Physical Chemistry C.* **113** (11), 4277-4285 (2009).

59. Schurtenberger, P., & Newman, M. E. Characterization of biological and environmental particles using static and dynamic light scattering in *Environmental Particles.* Vol. **2** (eds J. Buffle & H. P. van Leeuwen) 37-115 Lewis Publishers, (1993).
60. Jain, R. *et al.* Extracellular Polymeric Substances Govern the Surface Charge of Biogenic Elemental Selenium Nanoparticles. *Environmental Science & Technology.* **49** (3), 1713-1720 (2015).
61. Harewood, K., & Wolff, J. S. Rapid electrophoretic procedure for detection of SDS-released oncorna-viral RNA using polyacrylamide-agarose gels. *Anal. Biochem.* **55** (2), 573-581 (1973).
62. Penfold, J., Staples, E., Tucker, I., & Thomas, R. K. Adsorption of mixed anionic and nonionic surfactants at the hydrophilic silicon surface. *Langmuir.* **18** (15), 5755-5760 (2002).
63. Krozer, A., & Rodahl, M. X-ray photoemission spectroscopy study of UV/ozone oxidation of Au under ultrahigh vacuum conditions. *J. Vac. Sci. Technol. A-Vac. Surf. Films.* **15** (3), 1704-1709 (1997).
64. Vig, J. R. UV ozone cleaning of surfaces. *J. Vac. Sci. Technol.* **3** (3), 1027-1034 (1985).
65. Sauerbrey, G. Verwendung von Schwingquarzen zur Wägung dünner Schichten und zur Mikrowägung. *Zeitschrift Fur Physik.* **155** (2), 206-222 (1959).
66. Introduction and QCM-D Theory - Q-Sense Basic Training. *Q-Sense - Biolin Scientific*, Boston University BioInterface Technologies (BIT) Facility, (2006).
67. Edvardsson, M., Rodahl, M., Kasemo, B., & Höök, F. A dual-frequency QCM-D setup operating at elevated oscillation amplitudes. *Anal. Chem.* **77** (15), 4918-4926 (2005).
68. Hovgaard, M. B., Dong, M. D., Otzen, D. E., & Besenbacher, F. Quartz crystal microbalance studies of multilayer glucagon fibrillation at the solid-liquid interface. *Biophys. J.* **93** (6), 2162-2169 (2007).
69. Liu, S. X., & Kim, J. T. Application of Kelvin-Voigt Model in Quantifying Whey Protein Adsorption on Polyethersulfone Using QCM-D. *Jala.* **14** (4), 213-220 (2009).
70. Reviakine, I., Rossetti, F. F., Morozov, A. N., & Textor, M. Investigating the properties of supported vesicular layers on titanium dioxide by quartz crystal microbalance with dissipation measurements. *J. Chem. Phys.* **122** (20) (2005).
71. Voinova, M. V., Rodahl, M., Jonson, M., & Kasemo, B. Viscoelastic acoustic response of layered polymer films at fluid-solid interfaces: Continuum mechanics approach. *Phys. Scr.* **59** (5), 391-396 (1999).
72. Fischer, H., Polikarpov, I., & Craievich, A. F. Average protein density is a molecular-weight-dependent function. *Protein Sci.* **13** (10), 2825-2828 (2004).
73. Schuster, B., Pum, D., & Sleytr, U. B. S-layer stabilized lipid membranes (Review). *Biointerphases.* **3** (2), FA3-FA11 (2008).
74. Malmström, J., Agheli, H., Kingshott, P., & Sutherland, D. S. Viscoelastic Modeling of Highly Hydrated Laminin Layers at Homogeneous and Nanostructured Surfaces: Quantification of Protein Layer Properties Using QCM-D and SPR. *Langmuir.* **23** (19), 9760-9768 (2007).
75. Vörös, J. The Density and Refractive Index of Adsorbing Protein Layers. *Biophys. J.* **87** (1), 553-561 (2004).
76. Hillier, A. C., & Bard, A. J. ac-mode atomic force microscope imaging in air and solutions with a thermally driven bimetallic cantilever probe. *Rev. Sci. Instrum.* **68** (5), 2082-2090 (1997).
77. Horcas, I. *et al.* WSXM: A software for scanning probe microscopy and a tool for nanotechnology. *Rev. Sci. Instrum.* **78** (1), 013705 (2007).
78. Merroun, M. L., Rossberg, A., Scheinost, A. C., & Selenska-Pobell, S. XAS characterization of gold nanoclusters formed by cells and S-layer sheets of *B. sphaericus.* JG-A12. Annual Report Forschungszentrum Rossendorf - Institute for Radiochemistry, (2005).
79. Jankowski, U., Merroun, M. L., Selenska-Pobell, S., & Fahmy, K. S-Layer protein from *Lysinibacillus sphaericus.* JG-A12 as matrix for Au III sorption and Au-nanoparticle formation. *Spectroscopy.* **24** (1), 177-181 (2010).
80. Selenska-Pobell, S. *et al.* Magnetic Au nanoparticles on archaeal S-Layer ghosts as templates. *Nanomater. nanotechnol.* **1** (2), 8-16 (2011).
81. Caruso, F., Furlong, D. N., & Kingshott, P. Characterization of ferritin adsorption onto gold. *J. Colloid Interface Sci.* **186** (1), 129-140 (1997).
82. Ward, M. D., & Buttry, D. A. *In situ* interfacial mass detection with piezoelectric transducers. *Science.* **249** (4972), 1000-1007 (1990).
83. Höök, F. *et al.* Variations in coupled water, viscoelastic properties, and film thickness of a Mefp-1 protein film during adsorption and cross-linking: A quartz crystal microbalance with dissipation monitoring, ellipsometry, and surface plasmon resonance study. *Anal. Chem.* **73** (24), 5796-5804 (2001).
84. Wahl, R. PhD thesis, *Reguläre bakterielle Zellhüllenproteine als biomolekulares Templat.*, Technische Universität Dresden, (2003).
85. Jennings, T., & Strouse, G. Past, present, and future of gold nanoparticles in *Bio-Applications of Nanoparticles.* 34-47 Springer, (2007).
86. Beveridge, T., & Fyfe, W. Metal fixation by bacterial cell walls. *Can. J. Earth Sci.* **22** (12), 1893-1898 (1985).

